Histidine-Rich Glycoprotein Binds to Human IgG and C1q and Inhibits the Formation of Insoluble Immune Complexes

Nick N. Gorgani, Christopher R. Parish, Simon B. Easterbrook Smith, and Joseph G. Altin*

Division of Immunology and Cell Biology, The John Curtin School of Medical Research, Australian National University, Canberra, ACT 2601, Australia

Received October 14, 1996; Revised Manuscript Received March 10, 1997[⊗]

ABSTRACT: Purification of the complement component C1q from human serum using an established method resulted in the copurification of two 30 kDa proteins with an N-terminal sequence identical to human histidine-rich glycoprotein (HRG). Therefore, to explore the possibility that HRG can interact with C1q, we examined the ability of 81 kDa (native) and the 30 kDa proteins (presumably proteolytic N-terminal fragments of HRG) to bind to C1q, using both ELISA and optical biosensor techniques. Both forms of HRG were found to bind to the human complement component C1q and also to purified human and rabbit IgG by ELISA. Kinetic analyses of the HRG−C1q and HRG−IgG interactions using the IAsys biosensor indicate two distinct binding sites with affinities K_{d1} 0.78×10^{-8} M and K_{d2} 3.73×10^{-8} M for C1q, and one binding site with affinity K_d 8.5×10^{-8} M for IgG. Moreover, the fact that both native and 30 kDa HRG bind to C1q and to IgG suggests that the IgG and C1q binding regions on HRG are located in the 30 kDa N-terminal region of the HRG molecule. The Fab region of IgG is likely to be involved in the HRG−IgG interaction since HRG also bound to $F(ab')_2$ fragments with an affinity similar to that seen with the complete IgG molecule. Interestingly, the binding between HRG and IgG was significantly potentiated (K_d reduced from 85.0 to 18.9 nM) by the presence of physiological concentrations of Zn^{2+} (20 μM). Conversely, the presence of Zn^{2+} weakened the binding of HRG to C1q (K_d increased from 7.80 to 29.3 nM). Modulation of these interactions by other divalent metal cations was less effective with relative potencies being $Zn^{2+} > Ni^{2+} > Cu^{2+}$. An examination of the effect of native and 30 kDa HRG on the formation of insoluble immune complexes (IIC) between ovalbumin and polyclonal rabbit anti-ovalbumin IgG revealed that physiological concentrations of HRG can markedly inhibit IIC formation *in vitro*. The results show that human HRG binds to C1q and to IgG in a Zn^{2+}-modulated fashion, and that HRG can regulate the formation of IIC *in vitro*, thus indicating a new functional role for HRG *in vivo*.

It is well established that certain autoimmune diseases, such as systemic lupus erythematosus (SLE) and rheumatoid arthritis (RA), are associated with the production of autoantibodies (Mountz et al., 1994). Moreover, *in vitro* studies have shown that autoantibodies can be cross-linked with their cognate antigens to form insoluble immune complexes (IIC) (Sittampalam & Wilson, 1984a), which can precipitate in target tissues (e.g., joint synovial membrane) and lead to a lack of nutrient transport and consequent tissue injury. Evidence suggests that the effective clearance of circulating immune complexes is necessary to limit immune complex-mediated tissue injury (Charlesworth et al., 1982). Protective measures may include mechanisms which inhibit IIC formation, as well as those which promote solubilization of formed IIC.

Evidence suggests that the complement components C3b and C1q can modulate the formation of IIC, *in vitro*. Upon activation of the complement cascade, the generation of complement C3b and its covalent binding to the Fc (Cγ2 or hinge domains) and/or Fab portion of the IgG molecule may both inhibit the formation of IIC and promote their solubilization (Anton et al., 1994; Schifferli, 1987; Takata et al., 1984). In contrast, C1q (a constituent of the C1 component of complement) is reported to enhance the formation of IIC by binding to IgG molecules via the Cγ2 domain (Burton et al., 1980) and may lead to the cross-linking of IgG molecules (Geronski et al., 1985; Easterbrook-Smith et al., 1988). The interaction of C1q with the Fc region of IgG molecules in immune complexes may also activate the complement cascade by the classical pathway (Schifferli, 1987). In addition, C1q is reported to bind to specific receptors on normal endothelial cells through its collagen-like fragment and to act as an Fc receptor for circulating IgG immune complexes (Zhang et al., 1986). In contrast, studies on the anti-opsonic effect of serum suggest that C1q inhibits the interaction between IgG and the Fc receptors on neutrophils (Hakansson et al., 1982).

In order to compare the effects of rabbit and human C1q on the formation of IIC between ovalbumin and rabbit anti-ovalbumin IgG *in vitro*, we recently purified rabbit and human C1q using an established method. During these studies, two proteins with an N-terminal sequence identical to histidine-rich glycoprotein (HRG) copurified with C1q (Gorgani et al., unpublished observation), suggesting that C1q may form a complex with this protein. Preliminary data also suggested that HRG may associate with IgG molecules. HRG

* To whom correspondence should be addressed at the Division of Biochemistry and Molecular Biology, The Faculty of Science, Australian National University, Canberra, ACT 0200, Australia. Phone: 61 (6) 249 4495. FAX: 61 (6) 249 0313. E-mail: Joseph.Altin@anu.edu.au.

[⊗] Abstract published in *Advance ACS Abstracts,* May 1, 1997.

S0006-2960(96)02573-1 CCC: $14.00 © 1997 American Chemical Society

is a 81 kDa protein present in human plasma at a concentration of 150 μg/mL, and was first described by Heimburger et al. (1972). The protein has since been isolated from the plasma of other species such as mouse, rabbit, cattle, and chicken. *In vitro* studies have implicated HRG in the divalent metal ion binding component of serum (Guthans & Morgan, 1982), regulation of the coagulation cascade (Leung et al., 1984; Leung, 1986), regulation of growth factor action (Brown & Parish, 1994), and regulation of immune function (Rylatt et al., 1981; Saigo et al., 1990; Chang et al., 1992; Olsen et al., 1996). Its precise physiological role, however, remains to be determined.

In this study, we used an enzyme-linked immunosorbent assay (ELISA) and the IAsys resonant mirror biosensor to study the binding of human HRG to human C1q and IgG, and to determine the kinetic constants for these interactions. In addition, we used light scattering techniques (Easterbrook-Smith et al., 1988) to examine the effects of human HRG and C1q on the formation of IIC between ovalbumin and polyclonal rabbit anti-ovalbumin IgG. The results show that physiological concentrations of HRG bind strongly to C1q and to IgG, and inhibit the formation of IIC *in vitro*, suggesting a previously undescribed functional role for HRG.

MATERIALS AND METHODS

Reagents. Human IgG, human C1q, bovine serum albumin (BSA, fraction V), ovalbumin (grade V), and polyoxyethylenesorbitan monolaurate (TWEEN-20) were purchased from Sigma Chemical Co., St. Louis, MO. (Carboxymethyl)-dextran cuvettes for the IAsys biosensor, EDC [1-ethyl-3-[3-(dimethylamino)propyl]carbodiimide], NHS (*N*-hydroxysuccinimide), and ethanolamine were purchased from Fisons Applied Sensor Technology, Cambridge, U.K. The homobifunctional reagent bis(sulfosuccinimidyl) suberate (BS3), sulfosuccinimidyl 6-(biotinamido)hexanoate (NHS-LC-Biotin), and gentle Ag/Ab elution buffer (a cuvette regeneration buffer gentle to the dextran matrix) were purchased from Pierce, Rockford, IL.

Purification of Proteins. Human C1q was purified from human serum using Biorex-70 ion-exchange chromatography followed by Sephacryl S-300 gel filtration as previously described (Tenner et al., 1981). Reduced SDS−PAGE analysis demonstrated that purification of C1q by this procedure resulted in the copurification of two proteins of 32 and 34 kDa. The proteins were electrophoretically transferred onto a Problott PVDF membrane, and after staining with Coomassie Brilliant Blue, the 32 and 34 kDa bands were excised and subjected to N-terminal sequencing using an Applied Biosystems Inc. 473A model sequencer.

Native human HRG of molecular mass 81 kDa was purified from fresh human plasma by equilibrating a phosphocellulose column with loading buffer comprising 10 mM sodium phosphate (pH 6.8) containing 1 mM dithiothreitol (DTT), 1 mM ethylenediaminetetraacetic acid (EDTA), and 0.5 M NaCl. DTT, EDTA, and NaCl were added to the plasma at the indicated final concentrations as in loading buffer before the plasma was passed through the column. The column was extensively washed with loading buffer, and bound HRG was eluted using the same buffer containing 2 M NaCl as described previously (Rylatt et al., 1981). For some experiments (for interactions between HRG and immobilized C1q), HRG was purified using the loading buffer without DTT. The column was equilibrated with 10 mM sodium phosphate (pH 6.8) containing 1 mM EDTA and 0.5 M NaCl (loading buffer). The plasma was mixed with EDTA and NaCl at the indicated final concentrations as in the loading buffer and with 4-(2-aminoethyl)benzenesulfonyl fluoride hydrochloride (AEBSF) at 100 μg/mL and aprotinin (a trypsin inhibitor) at 2 μg/mL. The plasma was passed through the equilibrated column, and unbound protein was removed by extensive washing of the column with the loading buffer. Bound HRG was then eluted from the column using the same buffer containing 2 M NaCl. Since our results indicated that 30 kDa HRG copurifies with C1q, the C1q purification procedure also was used to purify the N-terminal 30 kDa fragment of HRG. Rabbit anti-ovalbumin IgG was purified from immunized rabbit serum by Na_2SO_4 precipitation and ion-exchange chromatography using a DEAE-Sephacel column. The IgG was collected from the break-through peak as described (Easterbrook-Smith et al., 1988).

SDS−PAGE. The purity of HRG preparations was checked by SDS−PAGE analysis which was carried out as described (Laemmli, 1970). Aliquots of HRG were boiled in either reduced or nonreduced sample buffer and electrophoresed on a 12.5% acrylamide gel. After electrophoresis, protein bands were identified by Coomassie Brilliant blue staining of the gel. The purity of the HRG preparations as judged by the intensity of the contaminating bands was always >95%.

Formation of Insoluble Immune Complexes. The formation of insoluble ovalbumin/anti-ovalbumin IgG immune complexes was carried out by incubating rabbit polyclonal anti-ovalbumin IgG in 0.01 M phosphate, pH 7.4, 0.15 M NaCl (PBS) containing 3 mM NaN_3 and different amounts of HRG and/or C1q for 5 min in a quartz reaction vessel (final volume 1 mL) maintained at 37 °C. The formation of IIC was initiated by the addition of ovalbumin at an equivalent antigen:antibody ratio. Since the absorbance due to light scattering of a suspension of particles is related to the average size of the particles, the formation of IIC was monitored by measuring the absorbance at 350 nm of samples using a Varian Cary-1 spectrophotometer as described (Easterbrook-Smith et al., 1988).

ELISA Assays. HRG (125 nM) was coupled for 1 h to Maxi-sorb ELISA trays in 0.1 M $NaHCO_3$ buffer (pH 9.0). The trays were blocked with 1% (w/v) BSA in PBS (PBS−BSA) and then incubated with C1q in PBS−BSA for 1 h. Bound C1q was detected using a monoclonal mouse anti-C1q antibody (BUS-1) followed by incubation with a HRP-conjugated sheep anti-mouse antibody and color development using *o*-phenylenediamine dihydrochloride (2.5 mg/mL) in a 0.05 M sodium citrate, 0.1 M sodium phosphate buffer (pH 5.0) containing 0.03% (v/v) hydrogen peroxide as substrate. The binding of C1q was dose-dependent in the concentration range tested (15−125 nM). Under these conditions, nonspecific binding was assessed using the mouse mAb anti-DNP-9 (a mAb to 2,4-dinitrophenyl) as a control. No significant level of nonspecific binding could be detected using the control mAb, indicating that the signal observed using the BUS-1 mAb reflects C1q specific binding.

A similar ELISA assay was also used to study the binding of rabbit anti-ovalbumin IgG to immobilized HRG. HRG-coupled Maxi-sorb ELISA trays were incubated with rabbit IgG (0.03−2 μM) in PBS−BSA overnight at room temperature. Bound IgG was detected using a HRP-conjugated polyclonal goat anti-rabbit antibody followed by color

development. Parallel experiments in which a HRP-conjugated polyclonal goat anti-sheep antibody was used instead of HRP-conjugated goat anti-rabbit antibody, or in which BSA was coated onto the wells instead of HRG, indicated that the binding was specific for HRG.

Determination of Binding Constants Using the Biosensor. An IAsys resonant mirror biosensor (Fisons Applied Sensor Technology, Cambridge, U.K.) (Cush et al., 1993; Buckle et al., 1993) with a (carboxymethyl)dextran sensing cuvette was used to determine the kinetic constants and affinities of the HRG−C1q and HRG−IgG interactions. Except where indicated, all experiments were performed in PBS containing 0.05% Tween-20 and 10 mg/mL BSA (PBS−BSA−T) and at a temperature of 25 °C. The BSA (1%, w/v) was included in the buffer to reduce nonspecific binding. The reaction vessel was stirred continuously by the aid of a propeller. Binding was measured at 2 s intervals, and the readout from the biosensor was in units of arc-seconds. Each binding reaction was routinely followed for 5 min. All binding experiments were performed in triplicate. The "Fast Fit" program supplied by Fisons was used to evaluate the kinetic constants (George et al., 1995).

(a) Coupling of Streptavidin or C1q to the Dextran Matrix. Streptavidin or C1q was coupled via ϵ-amino groups to the (carboxymethyl)dextran sensing surface of the IAsys biosensor cuvette using 1-ethyl-3-[3-(dimethylamino)propyl]-carbodiimide and *N*-hydroxysuccinimide (EDC/NHS) (Cush et al., 1993; Buckle et al., 1993). This was done by equilibrating the cuvette in PBS buffer containing 0.05% Tween-20 (PBS−T) and then reacting the cuvette with a mixture of EDC/NHS for 7 min. Unreacted EDC/NHS was washed away with PBS−T followed by three washes with 0.01 M sodium acetate buffer (for immobilization of streptavidin, the pH was adjusted to 4.5, and for C1q immobilization, the pH was adjusted to 5.0 using 2 M acetic acid). Streptavidin (50 μg/mL) or C1q (10 μg/mL) in the indicated acetate buffer was added to the cuvette and allowed to react with the activated carboxyl groups for 5 min. Uncoupled streptavidin or C1q was removed by washing with the apppropriate acetate buffer, and unreacted succinimidyl groups were blocked by incubating with ethanolamine (1 M, pH 8.5) for 2 min. The cuvette was washed 3 times with the appropriate acetate buffer, and then washed with PBS−T followed by a wash with 10 mM HCl to remove any noncovalently bound protein. Consistent with studies using other proteins [e.g., see George et al. (1995)], under these conditions there was no evidence that the 10 mM HCl wash affected the ability of the immobilized C1q to interact with soluble HRG since binding constants did not change significantly after repeated washing of the cuvette with 10 mM HCl, even when the first HCl wash of the cuvette was omitted to avoid possible denaturation of the immobilized C1q. Biosensor responses of ~500 arc-s for the immobilized streptavidin and 1800 arc-s for immobilized C1q were observed. According to the relationship provided by the manufacturer, these conditions resulted in the coupling of 3 ng of streptavidin and 11 ng of C1q per mm^2 of dextran surface.

(b) Biotinylation of Proteins and Binding to the Biosensor Surface. The proteins to be biotinylated were dissolved in PBS at a concentration of 1 mg/mL and then reacted with NHS-LC-biotin (1 mg/mL) for 30 min at room temperature. The reaction was stopped by the addition of Tris buffer (pH 8.0) to a final concentration of 100 mM. Unreacted biotin was removed by washing extensively (five cycles of concentration and dilution) in a Centricon 10 microconcentrator (Amicon, Inc., Beverly, MA), before storing the biotinylated proteins at −20 °C in small aliquots until use.

Biotinylated proteins (e.g., biotinylated HRG or biotinylated IgG) were coupled to the immobilized streptavidin. Biotinylated protein (50 μg/mL) in PBS−T (e.g., IgG or HRG) was added to the streptavidin-coupled dextran cuvette equilibrated in PBS−T, and allowed to bind to the immobilized streptavidin for 5 min. Nonspecifically bound biotinylated protein was removed by washing 3 times with PBS−T, followed by three washes with 10 mM HCl for 2 min (for three cycles).

(c) Binding of Protein Ligands to Proteins on the Biosensor Surface. Before immobilization of the biotinylated proteins on the streptavidin−dextran, nonspecific binding between the protein ligands and the streptavidin−dextran was assessed by the addition of different amounts of the protein ligands in PBS−BSA−T to the cuvette. Under these conditions, no significant level of nonspecific binding of any of the protein ligands used in this study could be detected.

Preliminary experiments were performed to establish the concentration range of each protein ligand suitable for kinetic analysis. PBS−T was added to the protein-coupled cuvette to establish a base line (5 min), and the protein ligand to be studied was then added in PBS−T at different concentrations. Binding of the ligand was studied by monitoring the association phase for 5 min. Subsequently, the cuvette was washed with PBS−T, and the dissociation phase was monitored for 5 min. Bound ligand was removed (cuvette regeneration) by washing with either 10 mM HCl or the gentle Ag/Ab elution buffer (Pierce). The base line was then reestablished after washing the cuvette with PBS−T. As previously, we found no evidence that the 10 mM HCl wash significantly affected the ability of the proteins to interact under these conditions.

(d) Evaluation of the Kinetic Constants. The IAsys biosensor was provided with a digital DECpc 450D$_2$LP computer. Data obtained with the biosensor were transferred directly to the "Fast Fit" program (Fison Applied Sensor Technology). This program uses an iterative curve-fitting to derive the observed rate constant and the maximum response at equilibrium due to ligand binding at the particular ligand concentration. The association of a soluble ligand with an immobilized macromolecule can be described by the pseudo-first-order equation $R_t = R_0 + E(1 - e^{-k_{obs}t})$, when only one binding site is available for the ligand (Cush et al., 1993). In this equation, R_t is the IAsys response at time t in units of arc-seconds (this is proportional to the concentration of ligand−protein complex at time t, $R_t \propto$ [ligand−protein]$_t$), R_0 is the IAsys response at time $t = 0$ in units of arc-seconds induced by the addition of the ligand solution to the buffer in the cuvette (this represents a net displacement of the biosensor signal, and its value is determined by the Fast Fit program for each binding curve analyzed, $R_0 \propto$ [ligand−protein]$_0$), E is the maximum IAsys response in units of arc-seconds due to bound ligand at equilibrium ($E \propto$ [ligand−protein]$_\infty$), and K_{obs} is the observed rate constant (termed k_{on} in Fast Fit) given by $k_{obs} = k_{off} + k_{on}$[ligand] (George et al., 1995). For two binding sites, the "Fast Fit" program uses the equation $R_t = R_0 + E_1(1 - e^{-k_{obs1}t}) + E_2(1 - e^{-k_{obs2}t})$ to derive the kinetic constants (Cush et al., 1993). In this equation, E_1 and E_2 are the maximum response at equilibrium due to binding of the ligand to the high- and low-affinity

binding site, respectively, and k_{obs1} and k_{obs2} represent the observed rate constants for the high- and low-affinity binding site, respectively. This equation assumes that, at equilibrium, the ligand−protein complex is stable; thus, the equilibrium line must be parallel to the starting base line ([ligand−protein]$_\infty$), and at least 80−90% of the data must be taken into account when fitting data to a curve for either single or double exponential binding.

A linear relationship between k_{obs} and ligand concentration was obtained when the binding data related to the interaction of HRG with immobilized C1q using the biosensor were fitted to the double exponential curve. Using this method, the k_{on} and k_{off} values for the interaction are given by the slope and *y*-intercept of the plot, respectively.

In some instances, the Fast Fit program was used to extrapolate the dissociation data to the base line for determination of the k_{off} (see below). Values of dissociation constants obtained by using the relationship $K_d = k_{off}/k_{on}$ were in good approximation with those obtained by Scatchard analysis of the extent of association (not shown). No linear relationship was obtained by plotting k_{obs} versus ligand concentration for the interaction of HRG to immobilized IgG, indicating that the data do not fit an exponential curve. Therefore, in these instances, similar to other kinetic analyses (George et al., 1995), the first region of the progress curve that best fits the single exponential term (assuming that thermodynamic equilibrium is reached) was used to evaluate the parameters for the highest affinity interaction. This was done by plotting $\ln\{[E - (R_t - R_0)]/E\}$ versus time and selecting the linear region of this plot.

RESULTS

Human C1q Copurifies with and Binds to HRG. Our preliminary studies showed that purification of the complement component C1q from human serum using an established procedure (Tenner et al., 1981) employing Biorex-70 ion exchange chromatography followed by Sephacryl S-300 gel filtration resulted in the copurification of a contaminating protein of 30−35 kDa molecular mass which migrated as a 32−34 kDa doublet under reducing conditions (see Figure 1). N-Terminal amino acid sequencing of the two protein bands seen under reducing conditions, after their electrophoretic transfer to PVDF membranes, indicated that the residues identified in the N-terminal sequence of both bands (VSPTDXSAV) were identical to those reported for the N-terminal sequence of HRG (VSPTDCSAV) (Koide et al., 1986). Since the purification of forms of HRG in this molecular mass range (Heimburger et al., 1972), presumably derived from the cleavage of native 81 kDa HRG by plasmin and kallikrein in serum, has been reported (Smith et al., 1985; Lijnen & Collen, 1983), these findings suggested that the 30−35 kDa protein copurified with C1q may be derived from the cleavage of native HRG (81 kDa) (see Figure 1) and that HRG may interact with C1q.

The possibility that C1q can interact with HRG was initially explored using an ELISA assay. Significant binding of soluble human C1q to 30−35 kDa and to 81 kDa (native) HRG, each immobilized onto the wells of a 96-well plate, was detected by the ELISA assay (data not shown). In order to validate these preliminary experiments, the strength of the interaction between HRG and C1q was studied using the IAsys biosensor. C1q was immobilized onto the biosensor cuvette using the EDC/NHS procedure, and the binding of

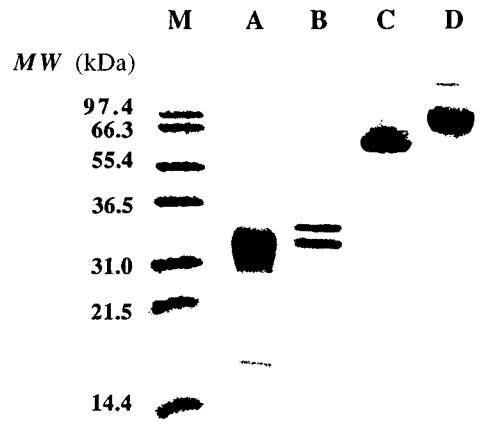

FIGURE 1: SDS−PAGE analysis of native HRG and 30 kDa proteins copurified with C1q. Native HRG and the 30 kDa proteins copurified with C1q were analyzed by SDS−PAGE (12.5% gel) under reduced and nonreduced conditions, and then stained with Coomassie Brilliant Blue. Lane M, reduced molecular mass marker proteins; lane A, nonreduced 30 kDa HRG; lane B, reduced 30 kDa HRG; lane C, nonreduced native HRG; lane D, reduced native HRG.

soluble HRG to the immobilized C1q was studied by adding different concentrations of HRG in PBS−BSA−T. The biosensor traces in Figure 2A show that the binding of soluble HRG to immobilized C1q over a 5 min period exhibits saturation kinetics with near-maximal binding occurring with 320 nM HRG (see Figure 2A). Under these conditions, no nonspecific binding of HRG to the dextran matrix could be detected (not shown). Analysis of the data obtained from these studies using the Fast Fit program indicated that the data did not fit to a single exponential function but that it could be fitted to a double expontential function, indicating that HRG reacts at two different sites on immobilized C1q with about 5-fold difference in affinity. The k_{off} and k_{on} for the higher affinity binding site were found to be $(1.04 \pm 0.57) \times 10^{-3}$ s^{-1} and $(1.39 \pm 0.095) \times 10^5$ M^{-1} s^{-1}, respectively. The dissociation constant for this interaction (as shown in Figure 2B and Table 1) as determined either by Scatchard analysis of equilibrium binding data (not shown) or by using the relationship $K_d = k_{off}/k_{on}$ was found to be $(0.78 \pm 0.46) \times 10^{-8}$ M. The k_{on} for the lower affinity binding site was determined from the slope of the plot shown in Figure 2B and found to be $(0.32 \pm 0.027) \times 10^5$ M^{-1} s^{-1}. The k_{off} value was obtained from the intercept of the plot shown in Figure 2B [$k_{off} = (3.60 \pm 2.30) \times 10^{-4}$ s^{-1}]. According to the manufacturer, k_{off} values in the range ($10^{-3} > k_{off} > 10^{-5}$ s^{-1}) need to be determined from the dissociation phase. Therefore, for the low-affinity binding site, the k_{off} value was determined by extrapolating the dissociation data to the base line and then fitting to a curve using the Fast Fit program (not shown). The k_{off} was similar for all concentrations of HRG tested; the average $k_{off} = (1.17 \pm 0.16) \times 10^{-3}$ s^{-1}. The dissociation constant as determined using $K_d = k_{off}/k_{on}$ was $(3.73 \pm 0.81) \times 10^{-8}$ M.

The binding of soluble C1q to immobilized HRG was studied also by immobilizing biotinylated HRG via streptavidin coupled to the dextran surface of the biosensor cuvette and adding C1q in solution at different concentrations in the range of 2.5−250 nM. The binding of soluble C1q to immobilized HRG over a 5 min period was dependent on the C1q concentration. There was no detectable nonspecific binding of C1q to the immobilized streptavidin (not shown). The binding was saturable at the higher C1q concentrations with

Table 1: Rate and Dissociation Constants for the Interaction of HRG with C1q and IgG/F(ab′)$_2$[a]

interaction	k_{on} (M^{-1} s^{-1}) × 10^{-5}	k_{off} (s^{-1}) × 10^{3}	K_d (M) × 10^{8}
HRG to immob C1q (high affinity)			
control	1.39 ± 0.095	1.04 ± 0.57	0.78 ± 0.46
+20 μM Zn^{2+}	1.25 ± 0.043	3.63 ± 0.88	2.93 ± 0.80
+20 μM Zn^{2+} and 1 mM EDTA	1.48 ± 0.078	0.68 ± 0.33	0.47 ± 0.25
HRG to immob C1q (low affinity)			
control	0.32 ± 0.027	1.17 ± 0.16[b]	3.73 ± 0.81
+20 μM Zn^{2+}	0.22 ± 0.014	0.79 ± 0.23[b]	3.67 ± 1.28
+20 μM Zn^{2+} and 1 mM EDTA	0.34 ± 0.020	1.35 ± 0.36[b]	4.05 ± 1.29
C1q to immob HRG	7.08 ± 0.19	6.4 ± 2.0	0.92 ± 0.30
HRG to immob IgG			
control	1.0 ± 0.054	8.60 ± 1.0	8.50 ± 1.50
+20 μM Zn^{2+}	1.40 ± 0.031	2.70 ± 0.67	1.89 ± 0.46
+20 μM Zn^{2+} and 1 mM EDTA	0.70 ± 0.033	13.0 ± 0.69	18.0 ± 1.83
HRG to immob F(ab′)$_2$	0.55 ± 0.029	4.70 ± 0.87	8.30 ± 1.7

[a] Kinetic constants were calculated by applying the "Fast Fit" program to the binding data obtained using the IAsys biosensor for the conditions indicated. In each instance, the constants represent the mean ± SEMs of three independent experiments. The set of data in control represent constants related to the interaction in PBS−BSA−T. [b] Off-rates (k_{off}) for these interactions were determined by using the dissociation phase.

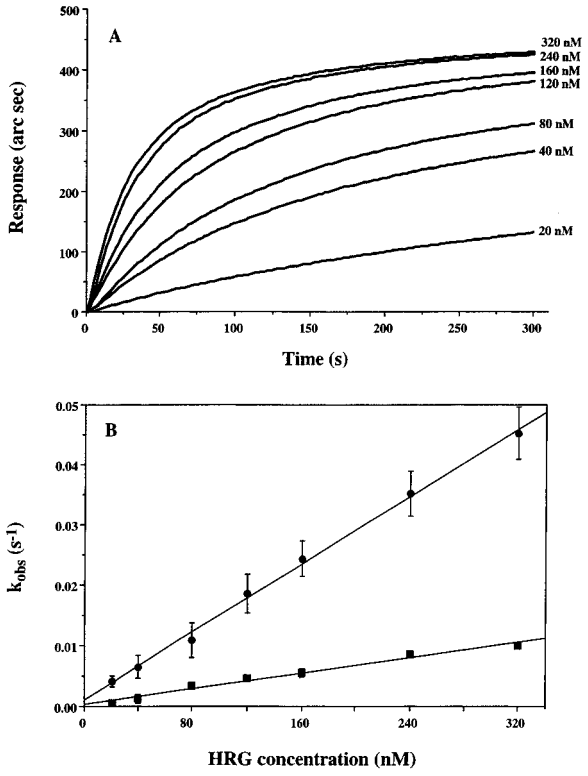

FIGURE 2: Determination of the binding constants for the binding of soluble HRG to immobilized C1q. The IAsys resonant mirror biosensor was used to study the binding of HRG to C1q immobilized onto the biosensor surface. After establishing a base line in PBS−BSA−T, the indicated concentration of HRG was added to the cuvette, and the association phase was monitored for 5 min. Overlay plots of the responses observed following the addition of different concentrations of HRG in the range of 20−320 nM are shown in (A). The cuvette was then washed with PBS−BSA−T, and the dissociation phase was monitored for 5 min (not shown). For each concentration of HRG, the values of $k_{obs(1)}$ and $k_{obs(2)}$ (rate constants) were determined by the linearization procedure using the Fast Fit program. As shown in (B), the plot of k_{obs} values related to high (●) and low (■) affinity binding sites against HRG concentration gives two straight lines with slopes of k_{on} and intercepts with the *y*-axis of k_{off}. Error bars show the ±SEM of triplicate experiments performed for each concentration of HRG; the absence of error bars indicates an error $<\pm 0.001$.

near-maximal binding occurring with about 250 nM C1q. The k_{on} and k_{off} for the reaction as determined using the Fast Fit program were found to be (7.08 ± 0.19) × 10^5 M^{-1} s^{-1} and (6.4 ± 2.0) × 10^{-3} s^{-1}, respectively, and the dissociation constant was (0.92 ± 0.30) × 10^{-8} M (see Table 1).

Human HRG Binds to IgG. The ability of HRG to bind to C1q with high affinity, and the reported ability of C1q to enhance the formation of IIC *in vitro*, prompted us to explore the possibility that HRG also binds to IgG. Preliminary experiments in which we examined the binding of polyclonal rabbit anti-ovalbumin IgG to immobilized human HRG using an ELISA assay indicated that HRG also interacts with rabbit IgG and that the binding is concentration dependent. A similar dose-dependent increase in the binding was observed when the F(ab′)$_2$ fragment of rabbit IgG was used instead of IgG, and when 30 kDa human HRG was used instead of native HRG (data not shown).

The HRG−IgG interaction was further studied with the biosensor using immobilized IgG. For these experiments, biotinylated human IgG was immobilized by binding to streptavidin coupled to the dextran surface, and the binding of different concentrations of HRG to the immobilized IgG was monitored over a 5 min period. The data in Figure 3A indicate that native human HRG binds to human IgG, and that the binding is concentration dependent in the range of 10−400 nM HRG. The binding was saturable with near-maximal binding occurring with 400 nM HRG. The k_{obs} value for the binding of each concentration of HRG was calculated using the linearization procedure and the Fast Fit program. The plot of k_{obs} against the corresponding HRG concentration is shown in Figure 3B and gives a straight line with a slope of k_{on} [(1.0 ± 0.054) × 10^5 M^{-1} s^{-1}] and an intercept with the *y*-axis of k_{off} [(8.6 ± 1.0) × 10^{-3} s^{-1}]. The dissociation constant was (8.5 ± 1.5) × 10^{-8} M (see Table 1).

Experiments also were carried out to study the binding of human IgG to immobilized human HRG. For these studies, the HRG was coupled to the dextran surface using the EDC/NHS procedure or via the biotin−streptavidin linkage (as above) or was chemically linked to a cuvette with an amino-silane surface using the amino-reactive homobifunctional cross-linker bis(sulfosuccinimidyl) suberate (BS3). Although the binding of C1q to HRG immobilized via the biotin−streptavidin linkage was fast, strong, and concentration dependent (see Figure 2A,B and Table 1), under these conditions no significant binding of soluble human or rabbit IgG to the immobilized HRG could be detected. Thus, it appears that the direct covalent cross-linking of the HRG to the biosensor cuvette, as well as linking the HRG via biotin−streptavidin, each can destroy the IgG binding site on the HRG.

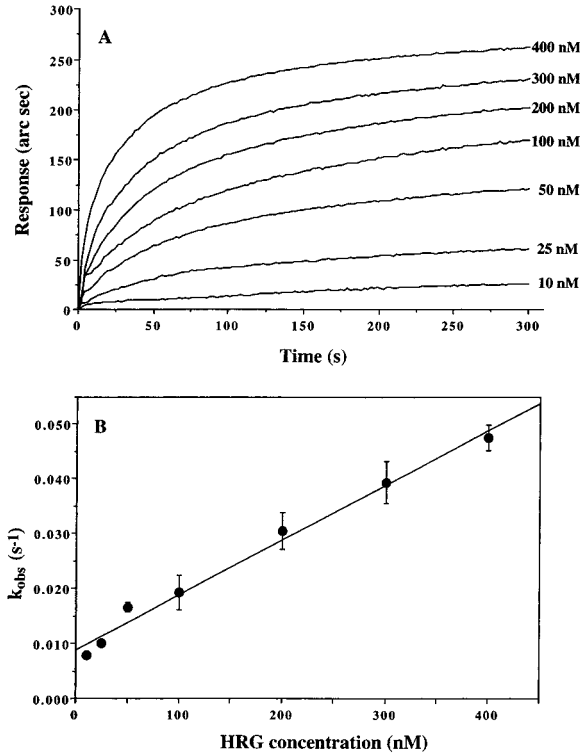

FIGURE 3: Determination of binding constants for the interaction of soluble HRG with immobilized IgG. The IAsys resonant mirror biosensor was used to study the binding of HRG to biotinylated human IgG immobilized onto the biosensor surface by coupling to immobilized streptavidin. The biosensor cuvette was equilibrated in PBS−BSA−T, HRG was added at the indicated concentrations, and the association phase was monitored for 5 min. The cuvette was then washed with PBS−BSA−T, and the dissociation phase was monitored for 5 min. The overlay plots for the different concentrations of HRG are shown in (A). The value of k_{obs} (rate constant) related to each concentration of HRG was determined by linearization using the Fast Fit program, and the results are shown in (B). The plot of k_{obs} against HRG concentration gives a straight line with a slope of k_{on} and an intercept with the *y*-axis of k_{off}. Error bars show the ±SEM of triplicate experiments performed for each concentration of HRG.

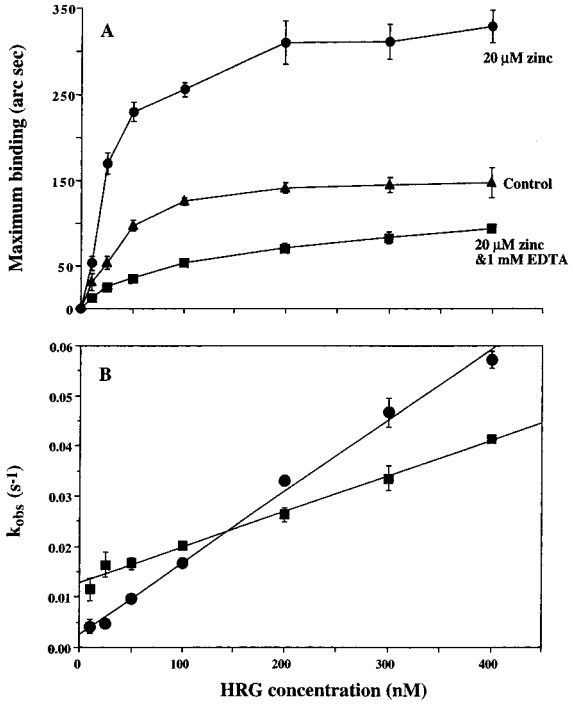

FIGURE 4: Effect of Zn^{2+} on the binding of native HRG to immobilized IgG. Pooled IgG (from human serum) was immobilized onto the biosensor surface, and the binding of HRG to the immobilized IgG was measured in the absence and presence of 20 μM Zn^{2+}. For each experiment, a base line was established in PBS−BSA−T plus 20 μM Zn^{2+} (PBS−BSA−T−Zn) for 5 min before adding HRG at the indicated concentration (in the same buffer). HRG binding was followed for 5 min, and the cuvette was washed with the same buffer before monitoring the dissociation phase (data not shown). For some experiments, a base line in buffer also containing 1 mM EDTA (PBS−BSA−T−Zn−EDTA) was obtained for 5 min before adding HRG in the same buffer. The interaction also was followed for 5 min before washing the cuvette with BSA−PBS−T−Zn−EDTA and monitoring the dissociation phase (data not shown). The maximum binding (in units of arc-seconds) versus ligand concentration is shown in (A). For each concentration of HRG, the rate constant (k_{obs}) was determined by linearization using the Fast Fit program. The measured k_{obs} values obtained from experiments carried out in PBS−BSA−T−Zn (●) and in the presence of 20 μM Zn^{2+} and 1 mM EDTA in the reaction buffer (■) were plotted against HRG concentration and are shown in (B). Error bars show the ±SEM of triplicate experiments performed for each concentration of HRG.

The biosensor also was used to investigate the binding of human HRG to immobilized F(ab′)$_2$ fragments of rabbit IgG. For these experiments, biotinylated F(ab′)$_2$ fragments were immobilized by binding to streptavidin coupled to the dextran cuvette, and HRG was added at a concentration range of 10−625 nM in PBS−BSA−T. As previously, the binding and dissociation of HRG were carried out for 5 min. A dose-dependent increase in the binding of HRG to F(ab′)$_2$ fragments was observed. After calculating the k_{obs} for each concentration of HRG using the linearization and Fast Fit program, the k_{on} and k_{off} of the reaction were found to be $(0.55 \pm 0.029) \times 10^5$ M^{-1} s^{-1} and $(4.70 \pm 0.87) \times 10^{-3}$ s^{-1}, respectively, and the dissociation constant was $(8.30 \pm 1.70) \times 10^{-8}$ M (see Table 1). This dissociation constant is similar to that observed with the whole IgG molecule.

Effect of Zinc Ions on the Binding of HRG to Human IgG and to C1q. HRG is reported to bind divalent metal cations like Zn^{2+}, which can alter the ability of HRG to interact with heparin and to bind to T cells and elicit T cell responses (Kazama & Koide, 1992; Olsen et al., 1996). To determine whether Zn^{2+} also can affect the ability of HRG to interact with IgG or with C1q, binding studies using the biosensor also were carried out in the presence of 20 μM added Zn^{2+}, with and without 1 mM EDTA. These studies showed that mixing the HRG (100 nM) with different concentrations of Zn^{2+} (2.5−20 μM) increases the binding of HRG to the immobilized human IgG. The increase was positively correlated with the amount of added Zn^{2+}, and the potentiation was $Zn^{2+} > Ni^{2+} > Cu^{2+}$ (not shown). As shown in Figure 4A, the presence of Zn^{2+} potentiated the binding of HRG to immobilized IgG by 2−3-fold. In contrast, the presence of 1 mM EDTA (probably by binding to trace metal ions in the PBS buffer) markedly reduced the binding compared to that seen in the absence of added Zn^{2+} (see Figure 4A, and compare Figures 3B and 4B). The on-rate of the interaction between HRG and immobilized IgG increased from $(1.0 \pm 0.054) \times 10^5$ M^{-1} s^{-1} in the absence of added Zn^{2+} (control) to $(1.40 \pm 0.031) \times 10^5$ M^{-1} s^{-1} in the presence of added Zn^{2+}. Similarly, the presence of Zn^{2+} decreased the off-rate from $(8.60 \pm 1.0) \times 10^{-3}$ to $(2.7 \pm 0.67) \times 10^{-3}$ s^{-1}. Collectively, these changes in the on- and off-rates produced by Zn^{2+} resulted in approximately a 5-fold increase in the affinity of HRG for IgG. Moreover, experiments carried out in the presence of Zn^{2+} and EDTA

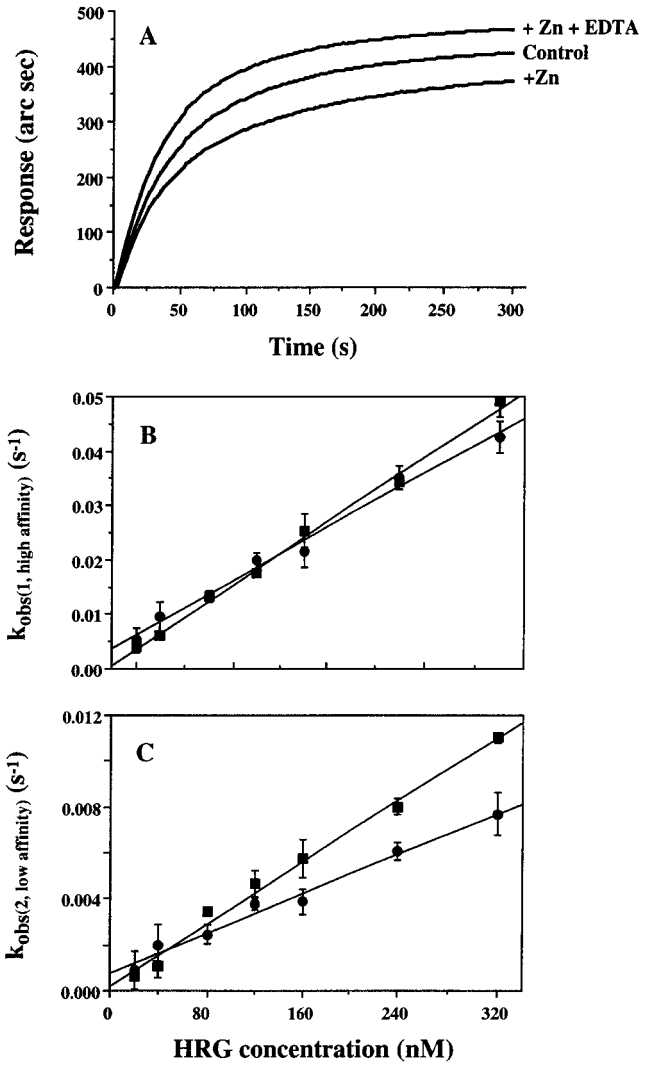

FIGURE 5: Effect of Zn^{2+} on the binding of native HRG to immobilized C1q. C1q was immobilized onto the biosensor surface, and the binding of HRG to the immobilized C1q was measured in the absence and presence of 20 μM Zn^{2+} as described in the legend of Figure 4. The association phase of the interaction (in units of arc-seconds) versus time (for 600 nM HRG) is shown in (A). For each concentration of HRG, the rate constants related to high ($k_{obs(1)}$) and low ($k_{obs(2)}$) affinity binding sites were determined by linearization using the Fast Fit program. The measured $k_{obs(1)}$ and $k_{obs(2)}$ values obtained from experiments carried out in PBS−BSA−T−Zn^{2+} (●) and in the presence of 20 μM Zn^{2+} and 1 mM EDTA in the reaction buffer (■) were plotted against HRG concentration and are shown for the high-affinity site in (B) and for low-affinity site in (C). Error bars show the ±SEM of triplicate experiments performed for each concentration of HRG.

indicated that the on-rate of the interaction was decreased from $(1.4 \pm 0.031) \times 10^5$ M^{-1} s^{-1} to $(0.70 \pm 0.033) \times 10^5$ M^{-1} s^{-1} by the addition of 1 mM EDTA. These experiments also showed that in the presence of EDTA the off-rate of the reaction was increased from $(2.70 \pm 0.67) \times 10^{-3}$ to $(13.0 \pm 0.69) \times 10^{-3}$ s^{-1}, and the dissociation constant was increased from $(1.89 \pm 0.46) \times 10^{-8}$ M to $(18.0 \pm 1.83) \times 10^{-8}$ M following the addition of the EDTA. The 2-fold reduction in the affinity of HRG for IgG produced by EDTA suggests that some metal ions may already be bound to the HRG, perhaps as a result of trace amounts of metal ions being present in the PBS used in these experiments.

Similar experiments carried out using immobilized C1q instead of IgG showed that, in contrast to the results observed with IgG, the affinity of HRG for immobilized C1q was decreased in the presence of 20 μM Zn^{2+}. At the two different HRG concentrations tested (50 and 600 nM), the inhibition of binding was dependent on the Zn^{2+} concentration (2.5−50 μM). Similar to the IgG−HRG interaction, the potency of inhibition was $Zn^{2+} > Ni^{2+} > Cu^{2+}$. As shown in Figure 5B,C and Table 1, the k_{on} for both binding sites was decreased in the presence of Zn^{2+}. In contrast, the presence of Zn^{2+} increased the k_{off} for the high-affinity binding site (determined from the association phase), but decreased the k_{off} for the lower affinity binding site (determined from the dissociation phase). Thus, compared to the control, approximately a 4-fold decrease in the high-affinity binding of HRG to immobilized C1q was observed in the presence of 20 μM Zn^{2+} (see Figure 5A,B,C and Table 1). In contrast, despite changes in the on- and off-rates, Zn^{2+} produced little change in the overall dissociation constant of the low-affinity interaction between HRG and immobilized C1q.

Effect of HRG, C1q, and Plasma on the Formation of Insoluble Immune Complexes. Our finding that HRG binds to C1q and to IgG led us to explore the possibility that HRG can modulate the formation of IIC. The effect of native and 30 kDa HRG on the formation of IIC between ovalbumin and polyclonal rabbit anti-ovalbumin IgG *in vitro* was investigated using light scattering techniques. Rabbit polyclonal anti-ovalbumin IgG was preincubated in a reaction vessel in PBS containing 3 mM NaN_3 and different concentrations of HRG and/or C1q for 5 min at 37 °C. The formation of IIC was initiated by the addition of ovalbumin at an equivalence antigen:antibody ratio, and the increase in particle size was monitored by measuring the absorbance at 350 nm as a function of time. Interestingly, the presence of either HRG preparation led to a dose-dependent decrease in the initial rate of formation of IIC. As shown in Figure 6A, preincubation of IgG with native HRG at a 1:1 molar ratio led to approximately a 50% inhibition in the absorbance within the first 5 min of the reaction. The data also show that both native and 30 kDa HRG increased the time to reach 50% maximum absorbance and that this increase is dependent on the HRG concentration (Figure 6B).

Experiments also were carried out to determine the effect of HRG on IIC formation in the presence of human C1q and plasma. As reflected by the increase in absorbance due to light scattering, preincubation of C1q with IgG led to an increase in the rate of IIC formation (Figure 6A). The time to reach 50% maximum absorbance was decreased in a dose-dependent manner by the addition of C1q (Figure 6B). Preliminary studies indicated that native HRG (75 μg/mL) did not affect IIC formation in the presence of C1q (12.5 μg/mL) (data not shown). As shown in Figure 7A, however, the formation of IIC was significantly inhibited when the IgG was preincubated with whole human plasma, and potentiated when preincubated with plasma in which the level of HRG was reduced to <10% of that in normal human plasma by passing through a phosphocellulose column as described (Rylatt et al., 1981). Furthermore, the potentiating effect of preincubating with the plasma containing reduced levels of HRG on IIC formation was abrogated when exogenous human HRG was included in the preincubations of this plasma with IgG (see Figure 7B). These findings are consistent with previous studies showing that C1q enhances the formation of IIC (Easterbrook-Smith, 1988), and suggest that the presence of HRG can inhibit the formation of IIC under physiological conditions.

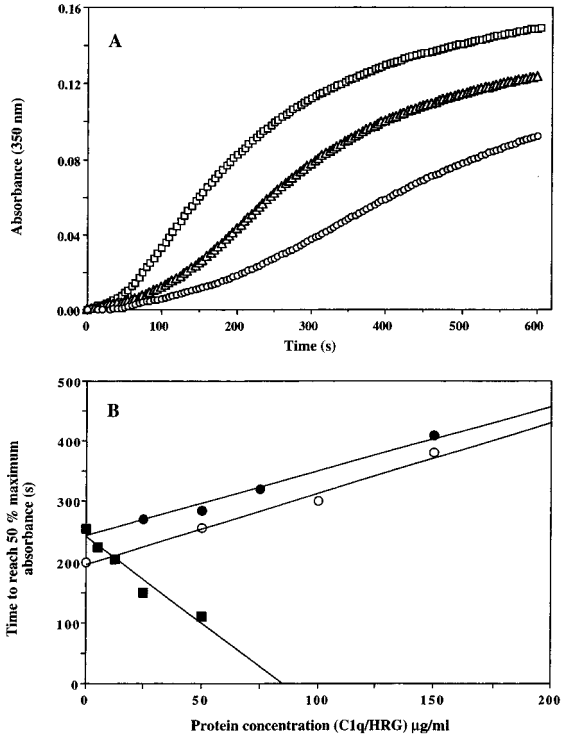

FIGURE 6: Effect of 30 kDa and native HRG and C1q on the formation of insoluble immune complexes. The formation of insoluble immune complexes was initiated by the addition of ovalbumin at an equivalence antigen:antibody ratio to a solution of IgG (175 μg/mL) preincubated with native HRG or C1q. To evaluate the inhibitory effect of 30 kDa HRG, the 30 kDa HRG was preincubated with a solution of IgG (200 μg/mL), and then ovalbumin was added at an equivalence antigen:antibody ratio. Immune complex formation was monitored as a function of time by measuring the absorbance at 350 nm associated with light scattering produced by the insoluble immune complexes that formed in the mixtures. The results in (A) show the increase in absorbance as a function of time due to formation of insoluble immune complexes for a control experiment (△, no additions), and for experiments carried out in the presence of 25 μg/mL C1q (□) and 150 μg/mL native HRG (○). The results in (B) show the time to reach 50% maximum absorbance as a function of the concentration of native HRG (●), 30 kDa HRG (○), or C1q (■). Each set of results is representative of five experiments performed in triplicate.

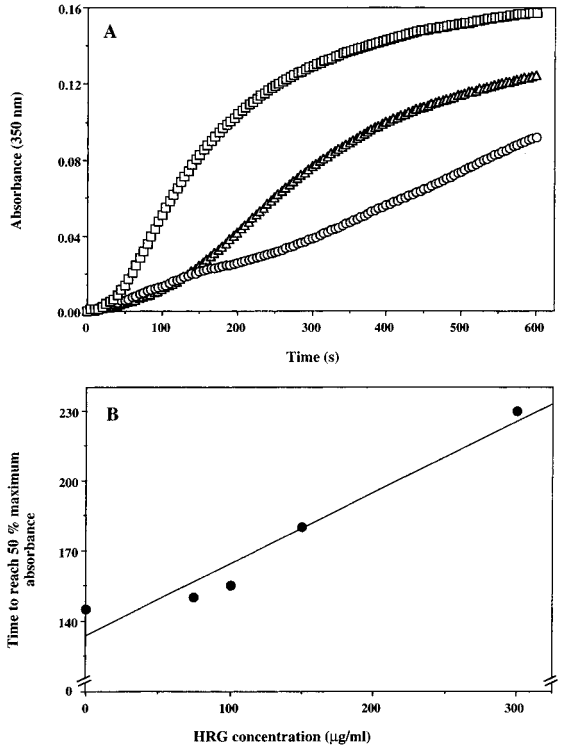

FIGURE 7: Effect of native human HRG on the formation of insoluble immune complexes in the presence of human plasma. The results in (A) show the absorbance change due to the formation of insoluble immune complexes which was initiated by the addition of ovalbumin to a solution of IgG (175 μg/mL, at equivalence antigen:antibody ratio) preincubated in PBS (△) or in PBS containing a 1 in 10 dilution of whole human plasma (○) or containing a 1 in 10 dilution of human plasma in which the levels of HRG were reduced to <10% of normal levels by phosphocellulose chromatgraphy (□). Immune complex formation was monitored as described in the legend to Figure 6. In addition, similar experiments were carried out in which the IgG was preincubated with plasma containing the reduced levels of HRG (at 1 in 10 dilution in PBS) and also containing the indicated concentration of added purified native HRG. Each point in (B) shows the time to reach 50% maximum absorbance, and is a representative result of three separate measurements performed at the indicated concentration of HRG.

DISCUSSION

The present study shows that HRG binds C1q and IgG with relatively high affinity compared to other HRG ligands (e.g., plasminogen and heparin) and, as a consequence, effectively inhibits the formation of IIC between ovalbumin and anti-ovalbumin IgG *in vitro*. The copurification of HRG with C1q was first reported by Haupt and Heimburger (1972), but they provided no evidence that the two proteins can interact. Furthermore, previous studies have shown that HRG purified from human serum consists of two identical 30 kDa subunits, held together by ionic interactions (Heimburger et al., 1972). In the present study, two bands of similar molecular mass (≈30 kDa) were observed to copurify with C1q, and N-terminal sequencing indicated that the two molecules have a N-terminal sequence identical to HRG. The possibility that C1q could bind to HRG was first suggested by our observation that the two 32−34 kDa contaminating proteins were not separated from C1q (400 kDa) by gel filtration on a Sephacryl S-300 column. These findings, therefore, provided evidence that C1q can interact with HRG.

The binding of HRG to immobilized human C1q was detected by optical biosensor techniques. The fact that biosensor data for the binding of HRG to immobilized C1q could be fitted to the double exponential relationship suggests that the binding of HRG to C1q occurs with two dissociation constants, namely, $(0.78 \pm 0.46) \times 10^{-8}$ M and $(3.73 \pm 0.81) \times 10^{-8}$ M. It would appear, therefore, that at least two distinct binding sites are involved in the HRG−C1q interaction. This notion is supported also by the dissociation phase in which, after the dissociation of the protein ligand from immobilized C1q (presumably from a lower affinity binding site), reassociation also could be detected (probably due to the rebinding of HRG to the higher affinity binding site) (not shown). The binding of human C1q to immobilized human HRG could be detected by ELISA and optical biosensor techniques. Kinetic studies of the binding of C1q to immobilized HRG using the biosensor showed the binding to have a dissociation constant of $(0.92 \pm 0.30) \times 10^{-8}$ M (see Table 1). The fact that the results indicate a single homogeneous response (i.e., no heterogeneous interactions) provides evidence either that hexameric C1q (Reid, 1974) is required to form the HRG binding site and/or that the tail region of the hexameric structure (as opposed to the head

region) is involved in the interaction with HRG. While a precise determination of the stoichiometry of the binding between HRG and C1q awaits the use of other techniques such as ultracentrifugation, the present results show that HRG and C1q interact with high affinity.

The present studies using ELISA and optical biosensor techniques also show that HRG binds to immobilized IgG, and the results are consistent with the previous observation that a trace amount of IgG is present in HRG preparations when the HRG is purified using (carboxymethyl)cellulose (Haupt & Heimburger, 1972). Biosensor analyses indicate that binding of soluble HRG to immobilized IgG is dependent on the concentration of soluble HRG and that the complex has a dissociation constant of $(8.50 \pm 1.50) \times 10^{-8}$ M (Figure 3A,B). Interestingly, a similar dissociation constant was observed when the $F(ab')_2$ fragment of rabbit IgG was used instead of whole IgG. Thus, the binding of HRG to immobilized $F(ab')_2$ was concentration-dependent, and the dissociation constant was $(8.30 \pm 1.70) \times 10^{-8}$ M (see Table 1). These findings suggest that HRG binds to IgG with a modest affinity resembling that of low-affinity Fc receptors (Van de Winkel & Anderson, 1991), and that the HRG−IgG interaction occurs predominantly via the Fab region of IgG. The IgG and C1q binding sites of HRG are likely to be located on the 30 kDa N-terminal domain of the HRG molecule since this domain interacted with both C1q and IgG in ELISA assays.

Although HRG interacts with immobilized IgG, no binding of human or rabbit IgG to immobilized HRG could be detected when the HRG was immobilized directly onto the biosensor surface using the homobifunctional cross-linking reagent BS3. Similarly, despite the fact that both native and biotinylated HRG bound to immobilized IgG with the same affinity, no binding of IgG to HRG could be detected when the HRG was immobilized by the biotin−streptavidin linkage, even if the first 10 mM HCl wash of the cuvette was omitted to avoid the possibility of denaturation of the HRG (data not shown). Additional studies showed that soluble HRG which had been exposed to 10 mM HCl for 5 min (before being neutralized with PBS) still retained its ability to bind to immobilized IgG in biosensor studies, and that IgG still bound to HRG when immobilized in an ELISA assay (not shown). The most likely explanation consistent with these observations is that the free ϵ-amino groups on the HRG involved in the biotinylation and cross-linking reaction are located close to the IgG binding region, and that this region is stearically hindered upon the immobilization of the HRG.

Consistent with our recent finding that physiological concentrations of Zn^{2+} potentiate the binding of HRG to T cells (Olsen et al., 1996), the present study shows that Zn^{2+} also potentiates the binding of HRG to IgG. The affinity of the binding of HRG to immobilized IgG was increased about 5-fold in the presence of a physiological concentration of Zn^{2+} (20 μM). Interestingly, the presence of added Zn^{2+} induced a 2-fold increase in the on-rate of HRG binding, but reduced the off-rate of the reaction to ~20% of that observed in the absence of added Zn^{2+}. These results suggest that the presence of Zn^{2+} leads to a faster and stronger interaction between HRG and human IgG. In contrast, the high-affinity binding of HRG to immobilized C1q was markedly inhibited by Zn^{2+} with the dissociation constant increasing from $(0.78 \pm 0.46) \times 10^{-8}$ M in the absence of added Zn^{2+} to $(2.93 \pm 0.80) \times 10^{-8}$ M in the presence of 20 μM added Zn^{2+}. The results suggest that Zn^{2+} can potentiate the ability of HRG to interact with some ligands (e.g., IgG) while at the same time inhibit the ability of HRG to interact with other ligands (e.g., C1q).

The mechanism by which Zn^{2+} potentiates the interaction between HRG and IgG is unclear. It has been shown that divalent metal cations like Zn^{2+} interact with the histidine−proline-rich domain of HRG (Morgan, 1985). Further studies have shown that protonation of the histidine−proline-rich domain of HRG transmits a conformational change to the rest of the molecule and may regulate its physiological function (Borza et al., 1996). In this study, the potencies of enhancement by other divalent metal ions such as Ni^{2+}, Cu^{2+}, or Zn^{2+} did not follow the lyotropic series but were more specific for Zn^{2+} and Ni^{2+} than for Cu^{2+}, suggesting that the binding of divalent cations to the HRG molecule does not depend only on charge−charge interactions. It is conceivable that a conformational change induced by the binding of Zn^{2+} may also explain the potentiation of the interaction between HRG and immobilized IgG.

Similarly, the inhibitory effect of Zn^{2+} on the binding of HRG to C1q may be due to a Zn^{2+}-induced conformational change in the HRG molecule which results in a reduced affinity for C1q. These features of the HRG molecule may also reflect its ability to regulate diverse physiological functions. Thus, the potentiation of the HRG−IgG interaction by Zn^{2+} may result in more effective inhibition of IIC formation, whereas the ability of Zn^{2+} to inhibit the HRG−C1q interaction may indicate an ability of HRG to regulate the classical complement pathway (see below).

A major finding from the present work is that physiological concentrations of either 30 kDa or native HRG can inhibit the formation of IIC between ovalbumin and polyclonal rabbit anti-ovalbumin IgG *in vitro*. This finding suggests that HRG may also play a role in regulating IIC formation *in vivo*, and is consistent with the observation that HRG is an acute phase reactant (Saigo et al., 1990). Our results indicate that 30 kDa HRG is as effective as native HRG in inhibiting IIC formation (Figure 6B), suggesting that the N-terminal region of HRG is involved in the interaction of HRG with IgG. Despite the fact that HRG binds to C1q with high affinity, in preliminary studies we were unable to detect any effect of HRG on IIC formation in the presence of C1q. A possible explanation for this latter observation is that other plasma proteins also are involved in regulating IIC formation. Alternatively, it is possible that the failure to detect any effect is due to the fact that a stirred reaction vessel was not employed in the present studies and C1q enhances IIC formation in the second phase of the progress curve when the IICs are larger than 100 nm in radii (Gorgani et al., 1996).

Interestingly, C3b is the only plasma protein previously reported to modulate the formation of IIC by covalently binding to the Fc and/or Fab region of IgG (Anton et al., 1994), and evidence suggests that this interaction may be an important factor in both inhibiting IIC formation and promoting solubilization of already formed IIC (Schifferli, 1987; Takata et al., 1984). C3b is produced, however, only after activation of the complement pathway which may result in the concomitant release of other complement proteins not involved in regulating IIC formation. Interestingly, it is also reported that HRG-depleted serum has less complement functional activity than whole serum (Chang et al., 1992).

This is consistent with the present studies suggesting that, whereas whole human plasma inhibits the formation of IIC in a dose-dependent manner, human plasma containing reduced levels of HRG (<10% of that in normal plasma) enhanced the formation of IIC (see Figure 7A). Moreover, the enhancement of IIC formation by plasma containing these reduced levels of HRG was inhibited by the addition of physiological concentrations of purified native HRG (Figure 7B). These observations suggest that HRG is a key plasma inhibitor of IIC formation and is able to inhibit this process in the presence of plasma proteins, thereby supporting the notion that this function of HRG is physiologically relevant.

Recently we showed that the process of formation of IIC can be divided into two phases (Gorgani et al., 1996). Initially the radii of the complexes increase slowly with time (during the process of insolubilization) until the average radius reaches a critical size (approximately 100 nm for ovalbumin and rabbit anti-ovalbumin IgG-containing immune complexes). This is followed by a phase of rapid increase in the radii (polymerization phase), leading to the formation of very large complexes. Interestingly, the enhancement of IIC formation by C1q occurs in the second phase of the progression curve when IgG-containing immune complexes are insoluble (Gorgani et al., 1996). The present study shows that HRG inhibits only the first phase of the progression curve when the mean radius of immune complexes is less than critical size and soluble IgG-containing immune complexes are present (not shown). The enhancing effect of C1q on IIC formation may not be physiologically relevent, therefore, if immune complexes are kept under critical size in radius by the noncovalent interaction of HRG with soluble IgG immune complexes in the early stages of disease or by the covalent binding of C3b to IgG immune complexes in chronic disease states.

It has been proposed that the production of autoantibodies may be responsible for the induction of immune complex diseases (ICD), e.g., rheumatoid factor (RF), against the IgG molecule in patients suffering from RA. It has also been shown that goat anti-human IgG and human IgG molecules can aggregate and insolubilize *in vitro* (Sittampalam & Wilson, 1984). In addition, Charlesworth et al. (1982) have shown that the effective clearance of circulating immune complexes is necessary to limit immune complex mediated tissue injury in a mouse model of infectious mononucleosis. These observations may imply that the clearance of circulating IIC (in early stages) is also necessary to limit IIC-mediated tissue injury in patients suffering from other ICD, such as RA or SLE. At the molecular level, inhibition of the insolubilization of soluble immune complexes [which can lead to the formation of very large hydrophobic particles (Gorgani et al., 1996)] may play an important role in the initiation and pathogenesis of the ICD. The mechanism by which IIC precipitate in target tissues (e.g., synovium of patients suffering from RA) is still unclear, although inhibition of the insolubilization process may be a factor which can limit this process and thus the pathogenesis of ICD.

ACKNOWLEDGMENT

Analysis and interpretation of the biosensor data were carried out with the expert assistance of Emeritus Prof. John Morrison (JCSMR).

REFERENCES

Anton, L. C., Ruiz, S., Barrio, E., Marques, G., Sanchez, A., & Vivanco, F. (1994) *Eur. J. Immunol. 24*, 599−604.
Borza, D.-B., Tatum, F. M., & Morgan, W. T. (1996) *Biochemistry 35*, 1925−1934.
Brown, K. J., & Parish, C. R. (1994) *Biochemistry 33*, 13918−13927.
Buckle, P. E., Davies, R. J., Kinning, T., Yeung, D., Edwards, P. R., Pollard-Knight, D., & Lowe, C. R. (1993) *Biosens. Bioelectron. 8*, 355.
Burton, D. R., Boyd, J., Brampton, A. D., Easterbrook-Smith, S. B., Emmanuel, E. J., Novotny, J., Rademacher, T. W., Van Schravendijk, M. R., Sternberg, M. J. E., & Dwek, R. A. (1980) *Nature 288*, 338−344.
Chang, N.-S., Leu, R. W., Rummage, J. A., Anderson, J. K., & Mole, J. E. (1992) *Blood 79*, 2973−2980.
Charlesworth, J. A., Endre, Z. H., Pussell, B. A., Yasmeen, D., & Peake, P. W. (1982) *J. Infect. Dis. 145*, 505−513.
Cush, R., Cronin, J. M., Stewart, W. J., Maule, C. H., Molloy, J., & Goddard, N. J. (1993) *Biosens. Bioelectron. 8*, 347−353.
Easterbrook-Smith, S. B., Vandenberg, R. J., & Alden, J. R. (1988) *Mol. Immunol. 25*, 1331−1337.
George, A. J. T., French, R. R., & Glennie, M. J. (1995) *J. Immunol. Methods 183*, 51−63.
Geronski, P., Bodenbender, L., Kanzy, E.-J., Loos, M., & Seiler, F. R. (1985) *Immunobiology 169*, 346−361.
Gorgani, N. N., Easterbrook-Smith, S. B., & Altin, J. G. (1996) *Biochim. Biophys Acta 1317*, 45−54.
Guthans, S. L., & Morgan, W. T. (1982) *Arch. Biochem. Biophys. 218*, 320−328.
Hakansson, L., Hallgren, R., & Venge, P. (1982) *Immunology 47*, 91−99.
Haupt, H., & Heimburger, N. (1972) *Hoppe-Seyler's Z. Physiol. Chem. 353*, S1125−1132.
Heimburger, N., Haupt, H., Kranz, T., & Baudner, S. (1972) *Hoppe-Seyler's Z. Physiol. Chem. 353*, S1133−1140.
Kazama, Y., & Koide, T. (1992) *Thromb. Haemostasis 67*, 50−55.
Koide, T., Foster, D., Yoshitaki, S., & Davie, E. W. (1986) *Biochemistry 25*, 2220−2225.
Laemmli, U. K. (1970) *Nature 227*, 680−685.
Leung, L. L. K. (1986) *J. Clin. Invest. 77*, 1305−1311.
Leung, L. L. K., Nachman, R. L., & Harpel, P. C. (1984) *J. Clin. Invest. 73*, 5−12.
Lijnen, H. R., & Collen, D. (1983) *Thromb. Res. 30*, 671−676.
Morgan, W. T. (1985) *Biochemistry 24*, 1496−1501.
Mountz, J. D., Wu, J., Cheng, J., & Zhou, T. (1994) *Arthritis Rheum. 37*, 1415−1420.
Olsen, H. M., Parish, C. R., & Altin, J. G. (1996) *Immunology 88*, 198−206.
Reid, K. B. M. (1974) *Biochem. J. 141*, 189−203.
Rylatt, D. B., Sia, D. Y., Mundy, J. P., & Parish, C. R. (1981) *Eur. J. Biochem. 119*, 641−646.
Saigo, K., Yoshida, A., Ryo, R., Yamaguchi, N., & Leung, L. L. K. (1990) *Am. J. Hematol. 34*, 149−150.
Schifferli, J. A. (1987) *Immunol. Lett. 14*, 225−228.
Sittampalam, G., & Wilson, G. S. (1984) *Anal. Chem. 56*, 2170−2175.
Smith, A., Nuiry, I., & Morgan, W. T. (1985) *Thromb. Res. 40*, 653−661.
Takata, Y., Tamura, N., & Fujita, T. (1984) *J. Immunol. 132*, 2531−2537.
Tenner, A. J., Lesavre, P. H., & Cooper, N. R. (1981) *J. Immunol. 127*, 648−653.
Van de Winkel, J. G. J., & Anderson, C. L. (1991) *J. Leuk. Biol. 49*, 511−524.
Zhang, S. O., Schultz, D. R., & Ryan, U. S. (1986) *Tissue Cell 18*, 13−18.

BI962573N